Supporting information

Design and construction of hollow metal sulfides/selenides core-shell heterostructure arrays for hybrid supercapacitor

Shuangxing Cui [a], Guochang Li [a], Xunwen Xiao [b,*], Lei Wu[a], Lei Han [a,*]

[a] State Key Laboratory Base of Novel Functional Materials and Preparation Science, School of Materials Science & Chemical Engineering, Ningbo University, Ningbo, Zhejiang 315211, China

[b] College of Material Science and Chemical Engineering, Ningbo University of Technology, Ningbo, Zhejiang 315211, China

* Corresponding Author. E-mail: xunwenxiao@nbut.edu.cn (Xiao); hanlei@nbu.edu.cn (Han)

Experimental

Materials:

Commercial nickel foam (NF, thickness: 1.7 mm, pore diameter distribution: 0.2–0.5 mm), hydrochloric acid (HCl,35–38%), cobalt chloride hexahydrate ($CoCl_2 \cdot 6H_2O$), nickel chloride hexahydrate ($NiCl_2 \cdot 6H_2O$), urea ($CO(NH_2)_2$), sodium sulfide ($Na_2S \cdot 9H_2O$), Lithium chloride (LiCl) and selenium dioxide (SeO_2) were obtained from Sinopharm Chemical Reagent Co., Ltd. All chemicals in the experiments were of analytical grade and used as received without any further purification.

Characterization:

We scrape the synthetic sample from the NF and use a magnet to suck up the nickel chips for all characterization. Crystal information of the sample was characterized by an X-ray diffractometer (XRD, Bruker D8 Advance) with Cu Ka radiation. The microstructure was characterized by scanning electron microscopy (SEM, Hitachi S-4800) and transmission electron microscopy (TEM, FEI TalosF200x). Elements analysis and valence states on the surface of products were characterized by X-ray Photoelectron Spectroscopy. The specific surface area was obtained by nitrogen adsorption-desorption with the Brunauer–Emmett–Teller (BET) model, and the pore size distribution was achieved by the Barrette-Joynere-Halenda (BJH) model. The types and contents of its elements are analyzed using energy dispersive spectroscopy (EDS) attached to a TEM device.

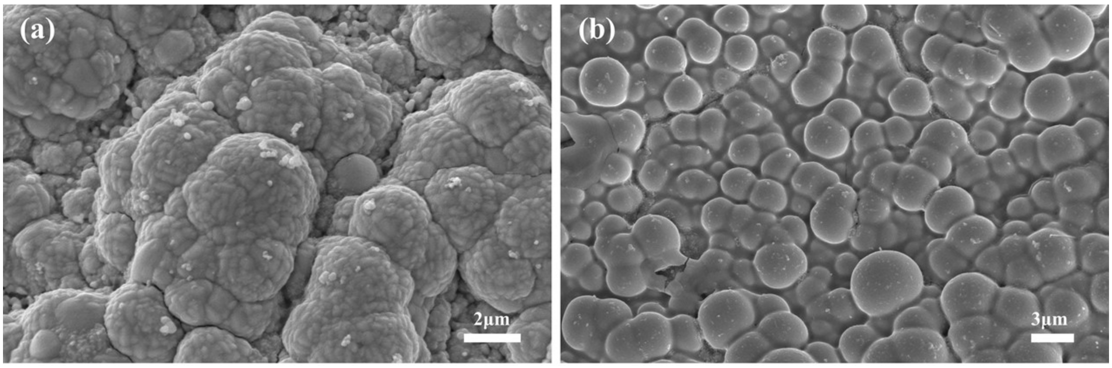

Fig. S1 SEM of (a) $NiSe_2$ and (b) $Co_{0.85}Se$.

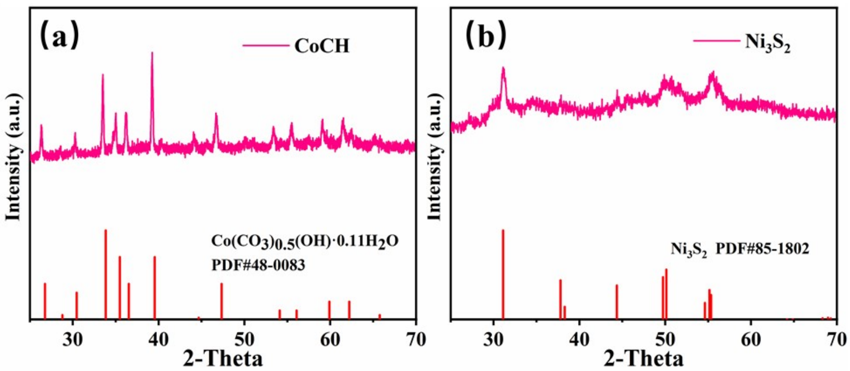

Fig. S2 XRD of (a) CoCH and (b) Ni_3S_2.

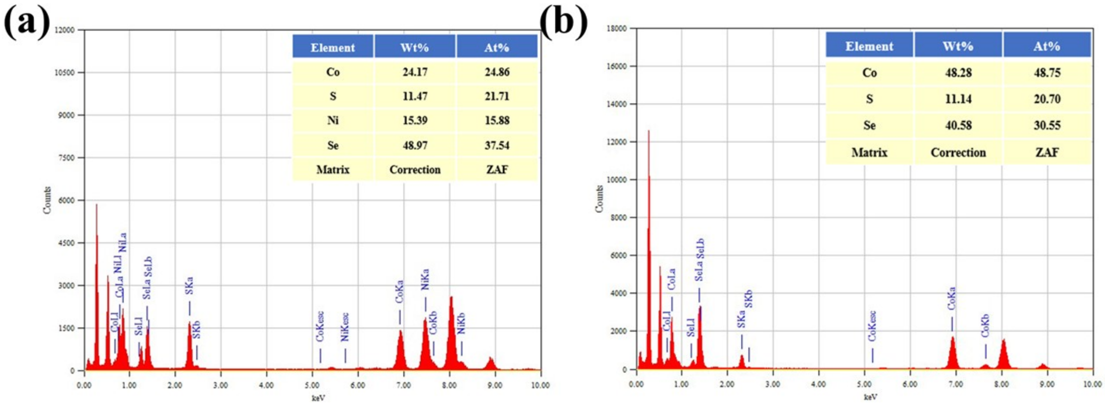

Fig. S3 EDS spectrum of (a) $NiSe_2@Co_9S_8$ and (b) $Co_{0.85}Se@Co_9S_8$.

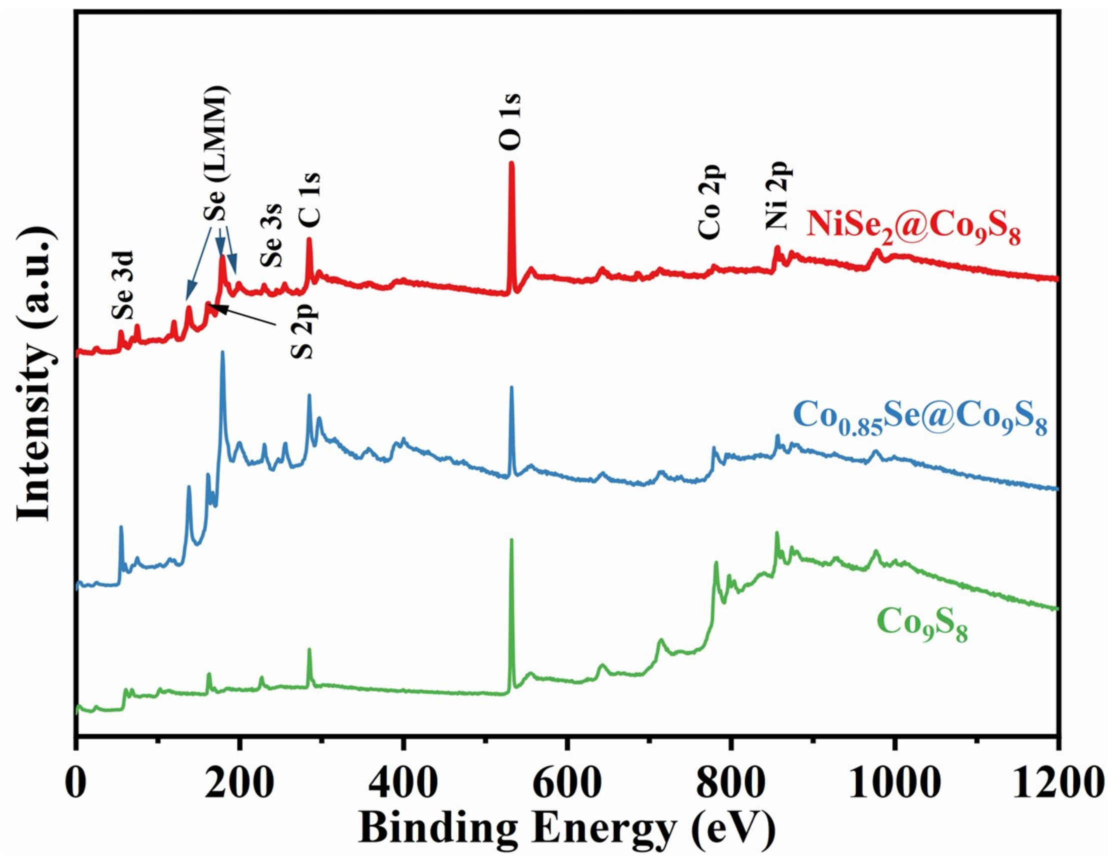

Fig. S4 XPS survey spectrum of $NiSe_2@Co_9S_8$, $Co_{0.85}Se@Co_9S_8$ and Co_9S_8.

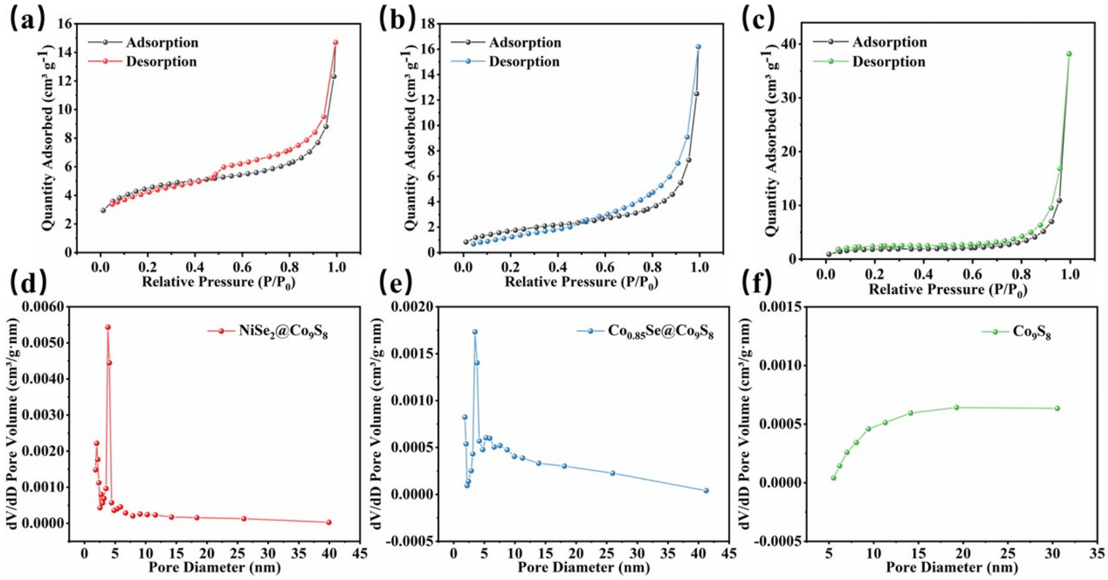

Fig. S5 Nitrogen adsorption-desorption isotherms of (a) $NiSe_2$@Co_9S_8, (b) $Co_{0.85}Se$@Co_9S_8 and (c) Co_9S_8; Pore diameter distribution of (d) $NiSe_2$@Co_9S_8, (e) $Co_{0.85}Se$@Co_9S_8 and (f) Co_9S_8.

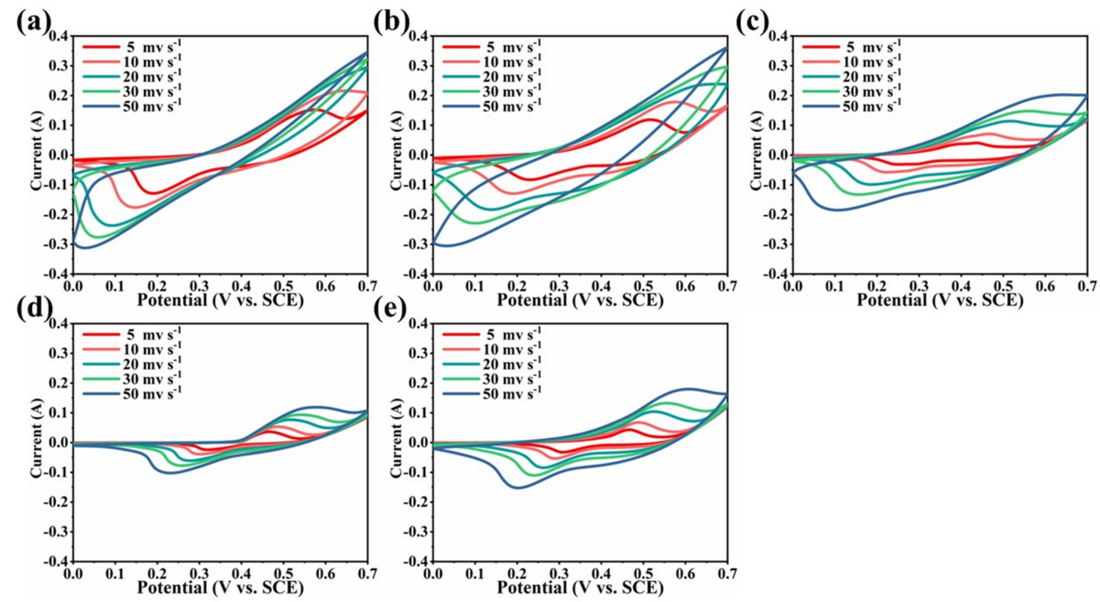

Fig. S6 CV curves of (a) $NiSe_2$@Co_9S_8, (b) $Co_{0.85}Se$@Co_9S_8, (c) Co_9S_8, (d) $NiSe_2$, and (e) $Co_{0.85}Se$ at different scan rates.

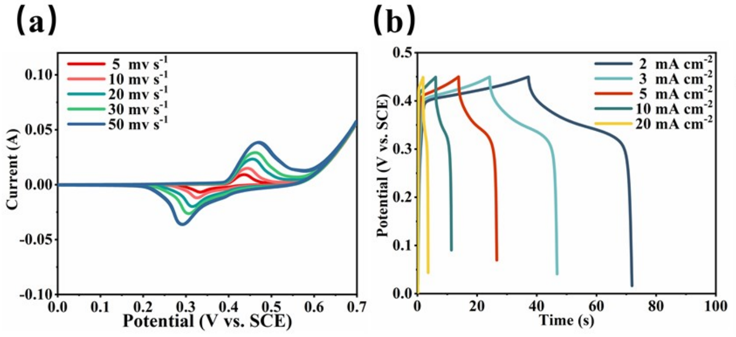

Fig. S7 (a) CV curves of Ni_3S_2 NF at different scan rates from 5 to 50 mV s^{-1}, (b) GCD curves of Ni_3S_2 NF at different current densities from 2 to 20 mA cm^{-2} and (c) areal capacity at different current densities of Ni_3S_2 NF.

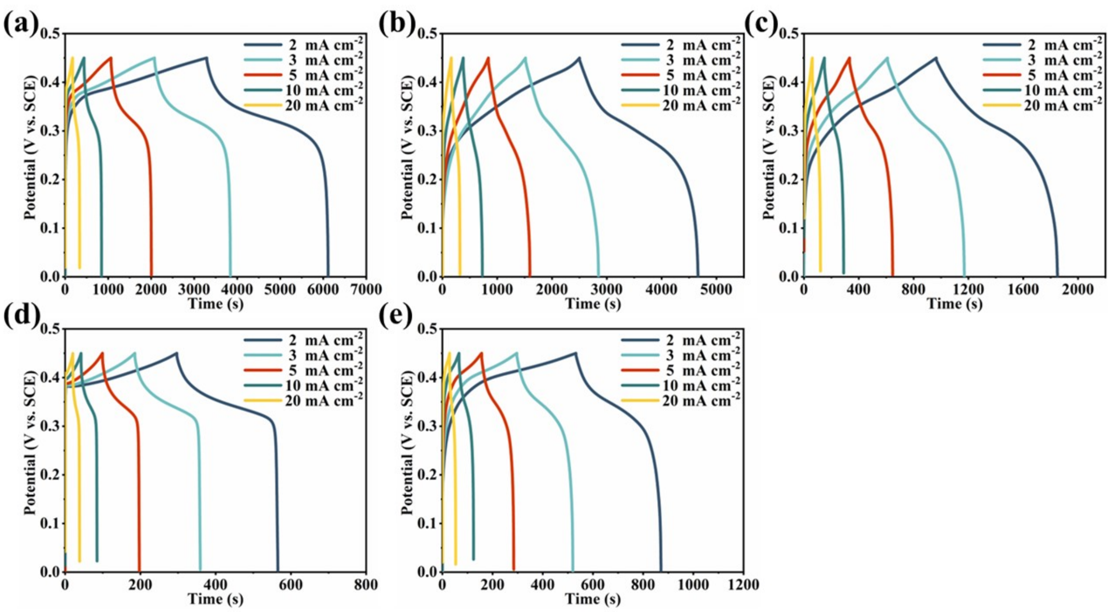

Fig. S8 CP curves of (a) $NiSe_2@Co_9S_8$, (b) $Co_{0.85}Se@Co_9S_8$, (c) Co_9S_8, (d) $NiSe_2$, and (e) $Co_{0.85}Se$ at different current densities.

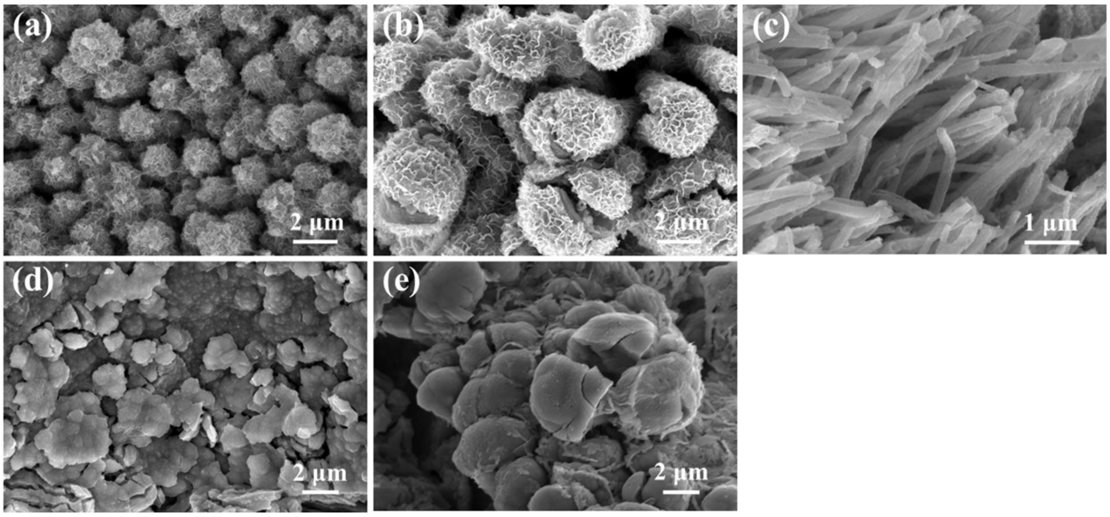

Fig. S9 SEM images of (a) $NiSe_2@Co_9S_8$, (b) $Co_{0.85}Se@Co_9S_8$, (c) Co_9S_8, (d) $NiSe_2$, and (e) $Co_{0.85}Se$ after 5000 cycles.

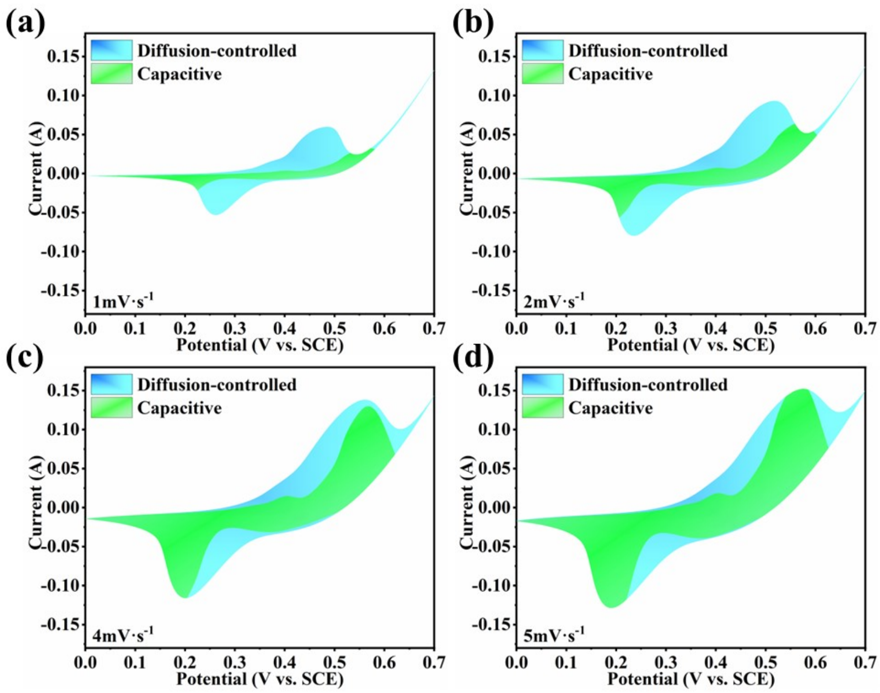

Fig. S10 CV curves of $NiSe_2@Co_9S_8$ with the capacitive and diffusion-controlled fraction shown by the shaded region at (a) 1 $mv\cdot s^{-1}$, (b) 2 $mv\cdot s^{-1}$, (c) 4 $mv\cdot s^{-1}$ and (d) 5 $mv\cdot s^{-1}$.

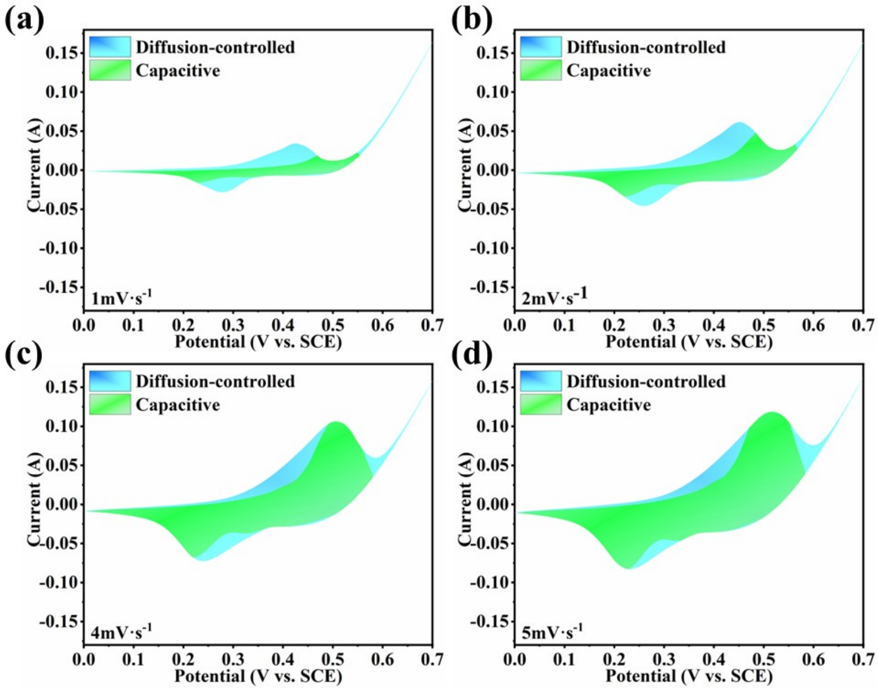

Fig. S11 CV curves of $Co_{0.85}Se@Co_9S_8$ with the capacitive and diffusion-controlled fraction shown by the shaded region at (a) 1 mv·s^{-1}, (b) 2 mv·s^{-1}, (c) 4 mv·s^{-1} and (d) 5 mv·s^{-1}.

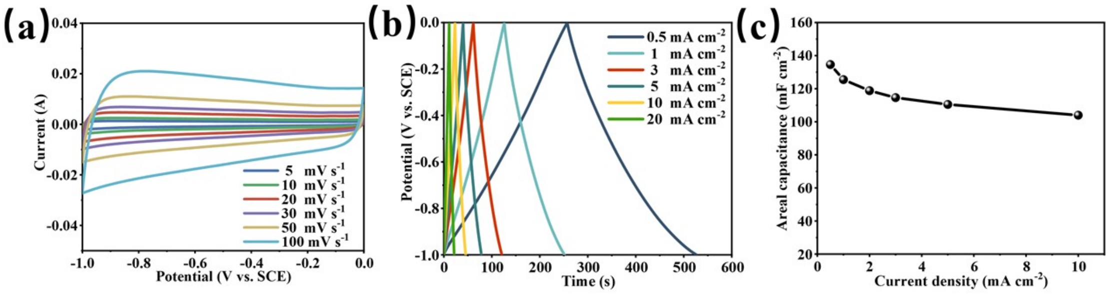

Fig. S12 (a) CV curves at different scan rates, (b) GCD curves at different current densities and (c) specific capacitance at different current densities of activated carbon.

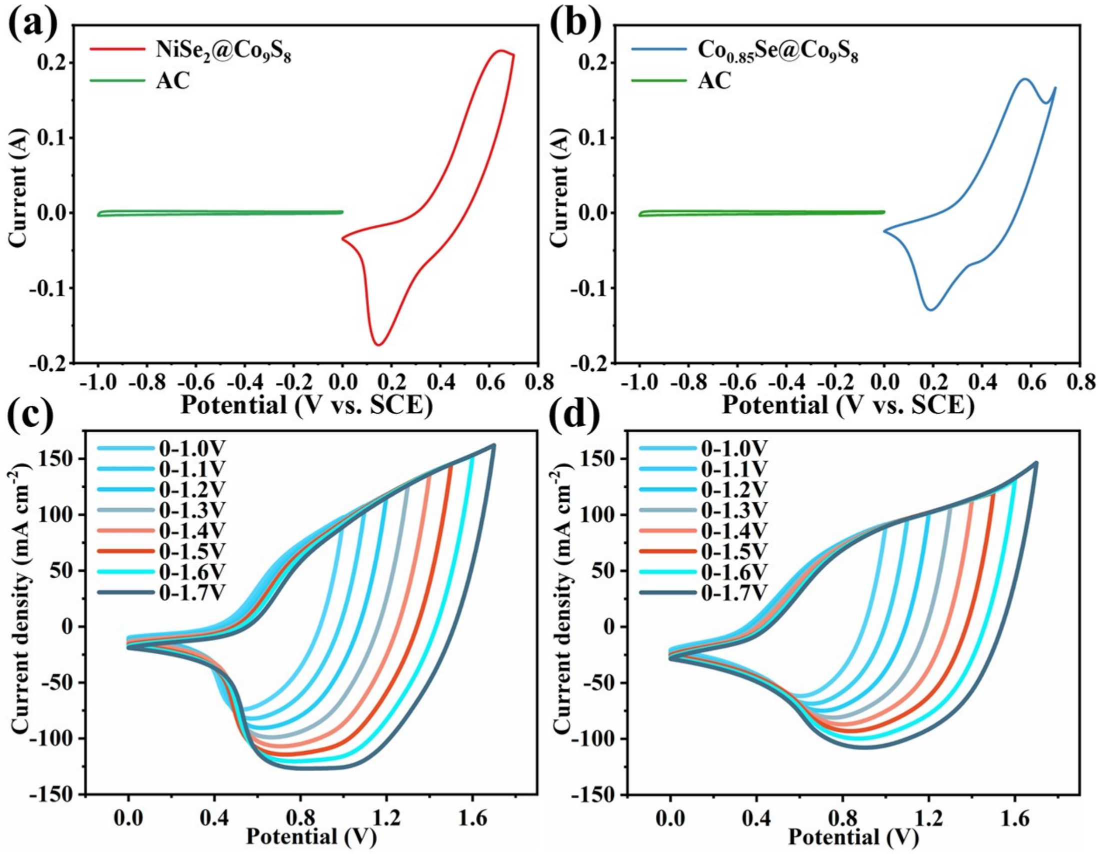

Fig. S13 CV curves of AC and (a) $NiSe_2$@Co_9S_8 and (b) $Co_{0.85}Se$@Co_9S_8 at 10 mV s^{-1} and CV curves of (c) $NiSe_2$@Co_9S_8//AC and (d) $Co_{0.85}Se$@Co_9S_8//AC in different potential windows at a scan rate of 50 mV s^{-1}.

Table S1 Performance comparison of supercapacitors.

Electrode materials	Capacitance	Current density	Electrolyte	Ref
$CoSe_2$@ZnS	953.3 F g^{-1}	1 A g^{-1}	3 M KOH	S1
$Co_{0.85}Se$@$CoNi_2S_4$/GF	5.25 F cm^{-2}	1 m A cm^{-2}	2 M KOH	S2
$NiSe_2$@CNT	980.5 F g^{-1}	1 A g^{-1}	6 M KOH	S3
Co_9S_8@MnO_2	3.7 F cm^{-2}	1 m A cm^{-2}	1 M Na_2SO_4	S4
Co_9S_8@NiMn oxide	5.34 F cm^{-2}	1 m A cm^{-2}	1 M LiOH	S5
NiSe/$Ni(OH)_2$	2725.69 F g^{-1}	5 m A cm^{-2}	3 M KOH	S6
NiSe nanoarrays	1.55 F cm^{-2}	4 m A cm^{-2}	1 M KOH	S7
NiSe@$NiCo(CO_3)(OH)_2$	6.89 F cm^{-2}	4 m A cm^{-2}	1 M KOH	S8
$NiCo_2Se_4$	6.21 F cm^{-2}	1 m A cm^{-2}	6 M KOH	S9
Ni_3S_2@Co_9S_8 nanotubes	8.24 F cm^{-2}	2 m A cm^{-2}	6 M KOH	S10
Co_3O_4/carbon foam	106 F g^{-1}	0.1 V s^{-1}	1 M NaOH	S11
Pr_6O_{11}@Ni-Co oxides	1635 F g^{-1}	0.5 m A cm^{-2}	2 M KOH	S12
$NiSe_2$@Co_9S_8	12.54 F cm^{-2}	2 m A cm^{-2}	2 M KOH	This work
$Co_{0.85}Se$@Co_9S_8	9.61 F cm^{-2}			

References

S1. S. A. Ahmad, M. Z. U. Shah, I. Hussain, M. Arif, P. Song, S. I. Al-Saeedi, M. Sajjad, I. Ahmad, J. Aftab, T. H. Huang and A. Shah, J. Energy Storage, 2023, **73**, 109090.

S2. C. Zhang, M. Hou, X. Cai, J. Lin, X. Liu, R. Wang, L. Zhou, J. Gao, B. Li and L. Lai, J. Mater. Chem. A, 2018, **6**, 15630-15639.

S3. Y. Y. Zheng, Y. R. Tian, S. Sarwar, J. J. Luo and X. Y. Zhang, J. Power Sources, 2020, **452**, 227793.

S4. Q. Li, M. Liu, F. Huang, X. Zuo, X. Wei, S. Li and H. Zhang, Chem. Eng. J., 2022, **437**, 135494.

S5. H. Qian, M. J. Liu, H. Zhang, X. Wei, H. Zhang, S. K. Li and F. Z. Huang, Electrochim. Acta, 2021, **399**, 139378.

S6. L. He, Y. Wang, Y. Guo, G. Li, X. Zhang and W. Cai, Nanotechnology, 2021, **32**, 345706.

S7. H. Chen, L. T. Wu, K. Y. Zhang, A. M. Qin and S. P. Chen, Int. J. Electrochem. Sci., 2018, **13**, 12437-12449.

S8. H. Gu, Y. Zeng, S. Wan, S. Zhang, Q. Zhong and Y. Bu, J. Mater. Chem. A, 2021, **9**, 16099-16107.

S9. R. Yang, Y. Zhang, X. Huang, H. Q. Yin, Y. Y. Mo, K. Y. Zhang, A. M. Qin, S. P. Chen and S. G. Dai, Ionics, 2023, **29**, 3353-3363.

S10. Y. Lin, X. Chen, P. Chang, Z. Liu, G. Ren and J. Tao, J. Alloys Compd., 2022, **900**, 163503.

S11. Z. Xu, A. Younis, D. Chu, Z. Ao, H. Xu and S. Li, J. Nanomater., 2014, **2014**, 1-5.

S12. N. Chen, A. Younis, S. Huang, D. Chu and S. Li, J. Alloys Compd., 2019, **783**, 772-778.